AIP | Journal of Applied Physics

# Compositional and structural changes at the anodic surface of thermally poled soda-lime float glass

E. C. Ziemath, V. D. Araújo, and C. A. Escanhoela

Citation: J. Appl. Phys. **104**, 054912 (2008); doi: 10.1063/1.2975996
View online: http://dx.doi.org/10.1063/1.2975996
View Table of Contents: http://jap.aip.org/resource/1/JAPIAU/v104/i5
Published by the AIP Publishing LLC.

# Compositional and structural changes at the anodic surface of thermally poled soda-lime float glass

E. C. Ziemath,[a] V. D. Araújo, and C. A. Escanhoela, Jr.
*Departamento de Física, IGCE, Universidade Estadual Paulista, Rio Claro, SP, CEP 13500-970, Brazil*

(Received 23 May 2008; accepted 1 July 2008; published online 11 September 2008)

Applying high dc electric fields at elevated temperatures on silicate glasses results in displacement of ions, causing compositional and structural changes in the anodic surface. In this work, the ionic displacement was accompanied by electric current measurements during poling. The thickness of the $Na^+$ depletion layer calculated from the current curves agrees with the thickness measured by EDS only if displacement of $Ca^{2+}$ and $O^-$ are also taken into account. A depletion of $Ca^{2+}$ in the anodic surface has in fact been observed. Structural changes were confirmed by infrared diffuse and specular reflectance spectroscopies. A narrowing of the band at about 1070 $cm^{-1}$ can be attributed to an increase in the structural ordering degree. Refractive index measurements confirm compositional changes and contact angle measurements indicate the existence of a negative charge density at the anodic surface. © *2008 American Institute of Physics*. [DOI: 10.1063/1.2975996]

## I. INTRODUCTION

Since the publication of the work by Myers *et al.*[1] about the capacity of optical second harmonic generation by thermally poled vitreous silica, there is increasing endeavor in finding glass compositions with nonlinear optical properties introduced after that procedure. Simultaneously, the interest and need in understanding the origin of such nonlinear properties, and how the structure and the chemical composition can intensify it have also heightened. In addition, aiming to optimize these properties, ideal poling conditions have been sought. Thus, several questions concerning this subject are still undetermined.

There is a general agreement that nonlinear effects originate in the layer immediately below the anodic surface, i.e., the surface of the glass that was in contact with the anode during the thermal poling procedure. Therefore this layer should undergo major chemical and structural changes, as for instance, the formation of a cation depleted layer, which seems to be responsible for the singular properties of thermally poled glasses. The formation of the cation depleted layer in silicate glasses containing alkalis, due to thermal poling, have been the focal point of several papers.[2–6]

The aim of the present work is to join supplementary information about the chemical and structural changes in the anodic surface of poled soda-lime silica glass, which might be helpful in clarifying the several observed physicochemical features that have been related to the formed depletion layer. The present work examines the compositional and structural changes in the anodic face of float glass samples submitted to different poling conditions. The most common techniques used for surface analysis have been employed: reflectance infrared spectroscopy and x-ray energy dispersive spectroscopy. Contact angle measurements were performed because an increase in the hydrofobicity of the anodic surface was observed. Electric current curves provide information about the time evolution of the depletion layer during poling. Refractive index measurements confirmed that the major chemical changes occurred in that surface.

## II. EXPERIMENTAL PROCEDURE

Thermal poling procedures were performed on commercially available 2.0 mm thickness float glass samples. The bulk composition of this glass, obtained by energy dispersive x-ray spectroscopy (EDS) measurements, is about (in wt %): 76.2 $SiO_2$, 10.3 $Na_2O$, 9.5 CaO, 3.4 MgO, 0.4 $MgO_2$, and 0.3 $K_2O$. These values are close to those generally found for this kind of glasses.[7] The experimental setup is shown schematically in Fig. 1. The samples were placed between 2.0 cm diameter stainless steel electrodes, inside an electric resistance furnace (EDG, mod. 1800 3P). Generally, an aluminum foil was placed between the anode and the glass surface to avoid adhesion between the steel electrode and the glass. The aluminum foil, when it adhered to the glass after the poling procedure, was removed with NaOH. The electrodes were connected to a high dc voltage power supply (Keithley, mod. 246). The applied voltage was about 2 kV in order to generate an electric field near 0.95–1.00 MV/m. A resistor of known value (~1 kΩ) was associated in series with the sample, and we measured the potential drop on this resistor

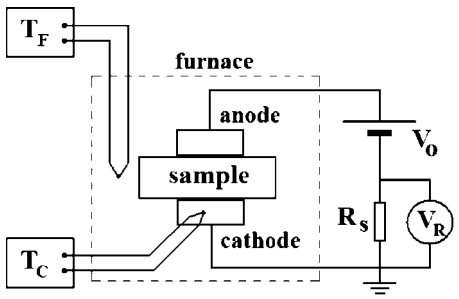


FIG. 1. Experimental setup for thermal poling. $V_O$: high voltage dc power supply; $V_R$: tension measured on known resistor $R_S$; $T_F$, $T_C$: temperatures of the furnace and the cathode/sample.

[a]Electronic mail: ziemath@rc.unesp.br.

 

to further calculate the electric current through the sample. The potential drop was measured with a digital voltmeter (Minipa-Appa, mod. ET-2609). Temperature was measured with *K* type thermocouples. One was placed near the sample and the other was fixed to the cathode with high-temperature silicone paste. High voltage was turned on only after the temperature of the cathode, and thus of the samples, had stabilized, which takes place about 1 h after the temperature of the furnace reaches the set one. Poling was performed at 180 and 250 °C, well below $T_g$ of the glass, which is about 560 °C. The electric current and the temperatures were simultaneously measured.

Float glass has the bottom face with some amount of tin, as a result of the fabrication process.[8–10] In this work, the top face, without tin, was placed in contact with the anode. In order to differentiate between the top and the bottom faces of float glass samples both surfaces were analyzed by optical microscopy after thermal treatment at 600 °C for 24 h. The surface without tin undergoes crystallization while that with tin presents the bloom effect.[8,11]

Measurements of the chemical composition changes in the glass due to the poling were performed by EDS (Link Isis, Oxford Instruments), coupled to a scanning electron microscope (DSM 940 A, Zeiss). Samples were metalized with a sputtered gold layer that was thin enough to allow the transmission of the elemental x-rays. The electrons were accelerated under a 15 kV voltage. The emission current of the filament was 80 $\mu$A.

Infrared spectra were obtained by diffuse reflection infrared Fourier transform (DRIFT) and specular reflectance modes. A Shimadzu spectrometer (FTIR-8300) with a diffuse reflectance device and a Perkin Elmer spectrometer (Spectrum 2000) with a specular device having adjustable incidence angle were employed. Aluminum mirror was used as reference in both cases.

Contact angle measurements were performed using a long working distance 5× objective of an optical microscope (Jenavert, Carl Zeiss/Jena). Milli-Q water drops of about 0.3 $\mu$l were deposited on the sample surface with a syringe. Due to the small volume of the drops, spherical caps were observed. The uncertainty in the contact angle measurement was about 2°.

The refractive index was measured with an Abbe refractometer (Carl Zeiss/Jena). A sodium vapor lamp was used as light source ($\lambda_D$=589.3 nm) and the refractometer was calibrated employing a BK7 optical glass ($n_D$=1.516 73). Before performing the measurements, a surface perpendicular to the main surfaces was sanded with 1000-mesh SiC particles. Optical coupling between the sample and the prism of the refractometer was obtained with $\alpha$-bromonaphtalene.

## III. RESULTS

The change in the electric current during a typical thermal poling procedure is shown in Fig. 2. As soon as the electric field is turned on, the current increases very fast. Further it increases slower up to a maximum and then decreases. This current increase is related to a temperature increase of the sample, which takes place immediately after the electric field is applied and is therefore attributed to the Joule effect. For lower poling temperatures, this increase is no longer observed because the initial value of the electric current is also reduced considerably. The temperature is delayed with respect to the current because the heat conduction up to the thermocouple fixed to the cathode takes some time. The maxima in the current curves shift to higher times with decreasing poling temperature. Light emission has been observed visually during poling. It has a faint bluish color and its intensity follows that of the current.

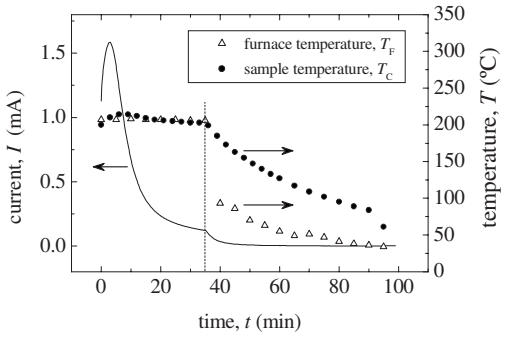


FIG. 2. Current curve obtained during thermal poling of float glass (2 kV, 200 °C). Furnace was turned off at 35 min.

The results of EDS measurements are presented in Fig. 3. The electron beam was moved along a straight line from outside the sample up to the exposed bulk, which causes the profile of all elements to have a sigmoidal shape at the interface, and this feature enables the estimation of the electron beam diameter to be about 1 $\mu$m. The changes in composition are observed mainly in the anodic surface [Fig. 3(a)].

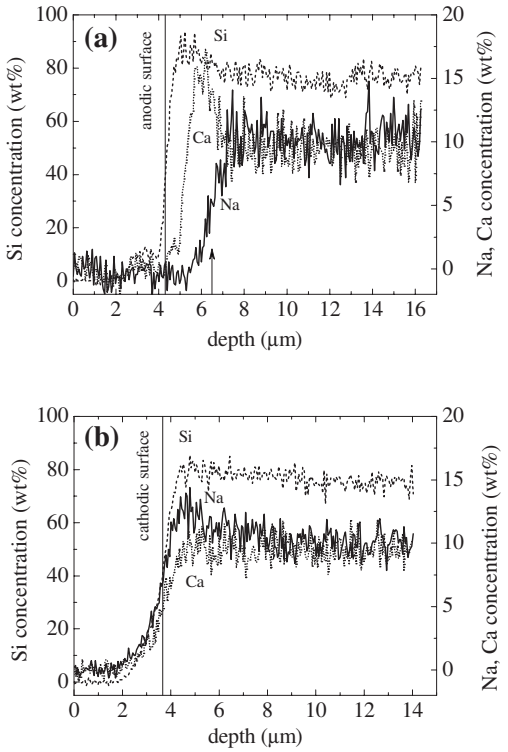


FIG. 3. Line-scan profile of Si, Na, Ca at the anodic (a) and cathodic (b) surfaces (poling conditions: 2 kV, 200 °C, 35 min). The arrow in (a) indicates the sodium depletion layer interface.

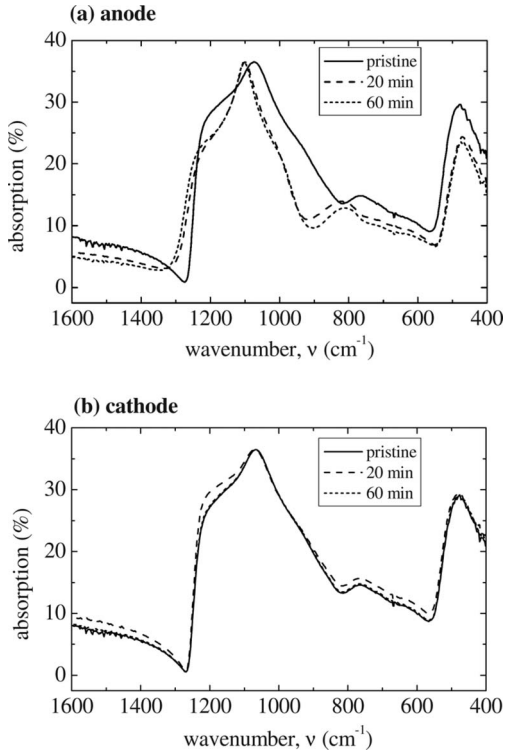


FIG. 4. DRIFT spectra of the anode and cathode surfaces superimposed to the spectrum of pristine glass surface. The spectra were normalized with respect to the band at 1070 $cm^{-1}$. Poling conditions: 20 and 60 min at 250 °C, 2 kV.

The increase in Si concentration is due to the absence of Na in the near surface region, known as the depletion layer. Under some poling conditions the concentration of $SiO_2$ can reach values as high as 94 wt % and that of $Na_2O$ vanishes. The thickness of this layer, in this case, is about 2 $\mu$m. The calcium profile shows that the ion of this element is also displaced into the bulk of the sample under the action of the strong electric field, leaving the anodic surface also partially depleted of calcium. According to Fig. 3(a), the Ca depletion layer has a thickness of about 1 $\mu$m. The profiles of the same elements in the cathode [Fig. 3(b)] show that the Si and Ca concentrations are unaltered with depth while that of Na indicates a small increase near the surface.

Infrared spectra were obtained in diffuse (DRIFT) and specular modes. Figure 4 shows diffuse reflectance spectra. The spectra of the anodic surface present the most pronounced changes when compared to that of the original glass surface. On the other hand, the spectra of the cathode surface are very similar to that of the original glass, indicating that no substantial chemical and structural change takes place at this surface.

Specular reflectance spectra are shown in Fig. 5. They confirm the more pronounced changes in the anodic surface. The cathodic surface spectrum presents little differences when compared to that of the original glass. The peak positions remain nearly the same with the angle of incidence, but an increase in the relative intensity of the shoulder at about 1200 $cm^{-1}$ was observed, which is generally noticed for other silicate glasses and for vitreous silica.[12–14] For the pristine and cathodic surfaces this shoulder becomes a more defined band only when the incident angle is higher than 60°. The bands at 1070 $cm^{-1}$ are narrower at the anodic surface. The bands at 816 $cm^{-1}$ at the anode correspond to the band at 764 $cm^{-1}$ of the pristine and cathodic surfaces.

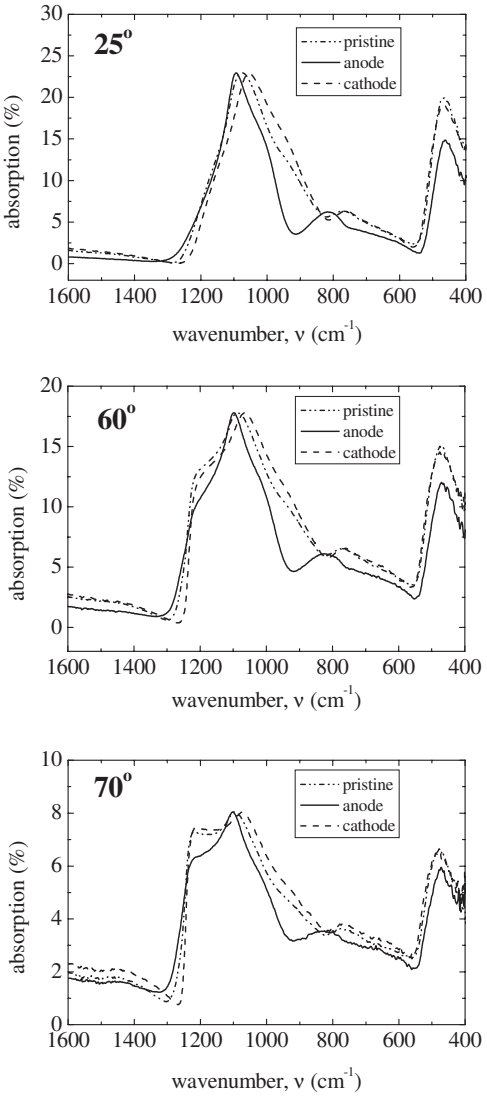


FIG. 5. Specular reflectance spectra of the anodic and cathodic surfaces taken at different incident angles and compared to that of the pristine glass. Spectra are normalized with respect to the bands in the range of 1070–1100 $cm^{-1}$. Poling conditions: 2 kV, 250 °C, and 20 min.

Figure 6 shows a water droplet deposited on the anodic surface of a poled glass sample, and the results of the mea-

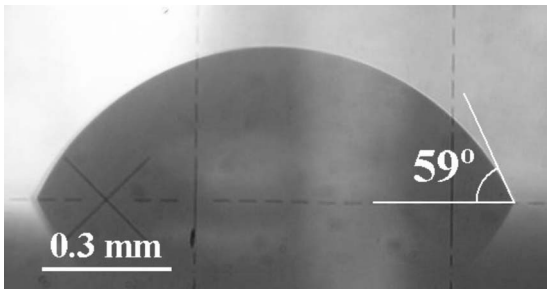


FIG. 6. A water droplet on the anodic surface of a 40 min poled glass at 250 °C and 2 kV.

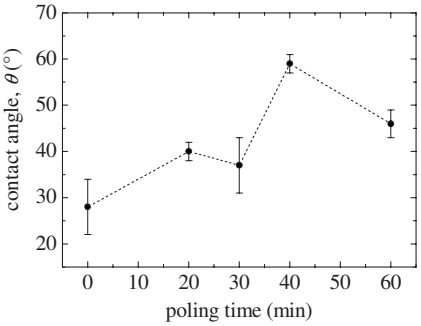


FIG. 7. Contact angle of the anodic surface for different poling times (poling conditions: 0.95 MV/m, 250 °C).

sured contact angles as a function of poling time are presented in Fig. 7. Measurements were not performed on the cathodic surface due to its high roughness.

The results of refractive index measurements are shown in Fig. 8, where a decrease with poling time can be observed for the anodic surface, while for the cathodic surface it is kept constant. The high uncertainty of the results presented in Fig. 8 is because the light-shadow interface observed in the refractometer is not sharp enough, which is attributed to the very small thickness of the depletion layer for this kind of measurement technique.

## IV. DISCUSSION

The electric current measured during poling is in principle attributed uniquely to the displacement of $Na^+$ ions under the action of the applied electric field. Consequently, the Na concentration at the anodic surface reduces with poling time and temperature, as confirmed by EDS measurements [Fig. 3(a)]. On the other hand, sodium accumulation would be expected near the cathodic surface unless it is expelled from the glass. In fact, the formation of a white powder layer was observed between the cathode and the glass surface, although some sodium is actually hindered near the cathodic surface, as shown by EDS profile measurements [Fig. 3(b)]. In order to identify the composition of this powder, EDS and infrared spectroscopy measurements were performed. Figure 9 presents scanning electron microscopy (SEM) image and EDS mapping of this white powder deposited on an aluminum foil placed between the cathode and the sample. Figure 9(b) shows that the white powder is rich in sodium. Infrared spectra of the powder deposited on the cathode and on the glass have much similarity to that of NaOH. The formation of this hydroxide is attributed to the reaction of metallic sodium, Na°, formed at the cathode, with atmospheric moisture after the sample has been cooled down to room temperature, while still inside the furnace.[6,15] Therefore, there are strong evidences that at least sodium is removed from the glass during poling.

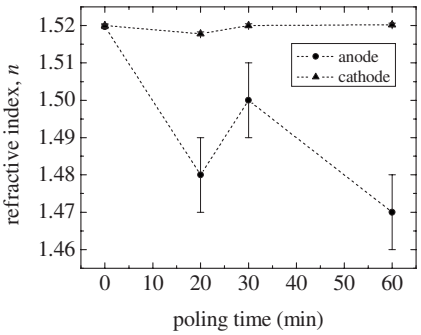


FIG. 8. Refractive index of the anodic and cathodic surfaces for several poling times (poling conditions: 0.95 MV/m, 250 °C).

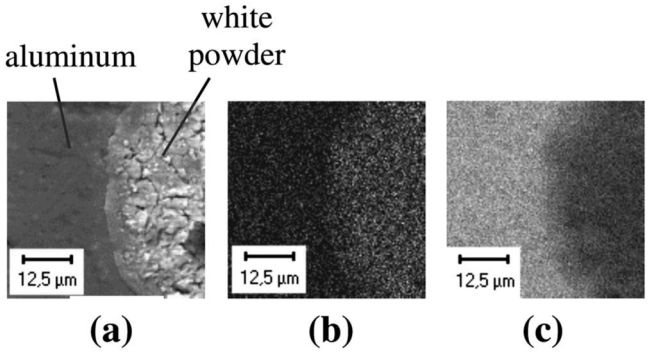


FIG. 9. (a) SEM image of the aluminum foil placed between the cathode and the sample after poling for 40 min at 150 °C. (b) and (c): EDS mapping of sodium and aluminum, respectively.

At the beginning of the poling process the electric field is uniformly distributed in the bulk of the sample and is responsible for the displacement of the most mobile ions, like $Na^+$, toward the cathode, under the action of a net electric force $F=eE_{bulk}$, as shown schematically in Fig. 10. Consequently, there is a fast increase in the electric current just after the high voltage is turned on (Fig. 2). Since the electrodes are perfectly blocking, a cation depletion layer is then gradually formed in the anodic region, which becomes negatively charged due to the increasing concentration of nonbridging oxygens, $Si-O^-$. The further increase in the current is related to the increase in the temperature due to the Joule effect. For lower poling temperatures, such increase is no longer observed. After reaching a maximum, the electric current begins to decrease as a consequence of the reduction in the electric field ($E_{bulk}$) outside the depletion layer. For very long poling times the negative charge in the depletion layer tends to equalize the positive charge in the anode hence reducing the electric current because $E_{bulk}$ vanishes. In this stage all the applied voltage drop will be mainly between the

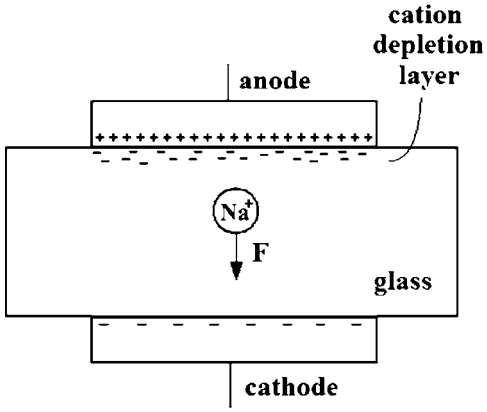


FIG. 10. Electric forces $F=eE_{bulk}$ acting on bulk cations. With increasing poling time, $E_{bulk}$ and the electric current tend to vanish.

anode and the depletion layer. The electric field in this layer becomes very high, with a magnitude of the order of 1 GV/m, considering a depletion layer thickness of 2 $\mu$m.

The thickness of the Na depletion layer, $l_d$, can be calculated by the following equation:

$$l_d = \frac{\int_0^t I(t)dt}{AeN_{\mathrm{Na}}}, \tag{1}$$

where $I(t)$ is the current (Fig. 2), $A$ is the electrode area, $e$ is the elementary charge, and $N_{\mathrm{Na}}$ is the Na concentration per unit volume in the glass. For this glass one has $N_{\mathrm{Na}} \cong 5.8 \times 10^{21}$ atoms cm$^{-3}$, taking into account that its density is 2.50 g cm$^{-3}$ and that its composition is that mentioned above. In the case of the current curve shown in Fig. 2(a), the calculated depletion layer thickness is 4.8 $\mu$m and the corresponding total electric charge displaced, $Q(t) = \int I(t)dt$, is 1.2 C. However, from EDS line-scanning measurements the corresponding thickness of the Na depletion layer, as shown in Fig. 3(a), is about 2 $\mu$m. These values show a substantial thickness difference for the same layer and this discrepancy was observed for all poling procedures. However, if the contribution of the displaced calcium is also taken into account, the denominator in Eq. (1) will increase, which lowers the calculated depletion layer thickness, but not enough to reach the measured value. The existence of a leakage current over the surface of the sample, which could increase the concentration of charge carriers, can be considered to explain an increase in charge carrier concentration, possibly leading to a smaller value of $l_d$ in Eq. (1), but in this case the measured current would not vanish so fast with time. Furthermore, the measured current intensity was not sufficiently high to characterize the existence of a leakage current. Another plausible explanation is that, in addition to the displacement of Na and Ca ions, oxygen ions, $O^-$, can move toward the anode, as already pointed out by Carlson.[2] The EDS is not sufficiently sensitive to perform a quantitative analysis of oxygen due to its low atomic number. However, it is possible to estimate the quantity of oxygen reaching the anode if one considers that one oxygen is produced for two sodium and another for one calcium according the reaction equations

$$\equiv \mathrm{Si} - \mathrm{O}^- \cdots \mathrm{Na}^+\mathrm{Na}^+ \cdots \mathrm{O}^- - \mathrm{Si} \equiv \rightarrow 2\mathrm{Na}^+ + \mathrm{O}^- + \equiv \mathrm{Si} - \mathrm{O} - \mathrm{Si} \equiv , \tag{2a}$$

$$\equiv \mathrm{Si} - \mathrm{O}^- \cdots \mathrm{Ca}^{2+} \cdots \mathrm{O}^- - \mathrm{Si} \equiv \rightarrow \mathrm{Ca}^{2+} + \mathrm{O}^- + \equiv \mathrm{Si} - \mathrm{O} - \mathrm{Si} \equiv , \tag{2b}$$

As a consequence, the concentration of charge carriers increases and, according to Eq. (1), the thickness of the calculated depletion layer will reduce even more. The concentrations of calcium and oxygen ions in the glass that are supposed to be involved in the electric current are, respectively, $N_{\mathrm{Ca}} \cong 2.4 \times 10^{21}$ and $N_{\mathrm{O}} \cong 5.3 \times 10^{21}$ atoms cm$^{-3}$. Therefore the calculated depletion layer is now $l_d \sim 1.6$ $\mu$m, which agrees better with the sodium depletion thickness measured by EDS. The total charge carriers ($Na^+$, $Ca^{2+}$, and $O^-$) can also be calculated from the values of the sodium and calcium depletion layer thicknesses: 2 and 1 $\mu$m, respectively. In these layers there are $3.7 \times 10^{18}$ $Na^+$ and $0.8 \times 10^{18}$ $Ca^{2+}$ cations and, according to Eqs. (2a) and (2b), also $5.3 \times 10^{18}$ oxygen ions will contribute with the measured electric current. These values lead to a total charge of 1.1 C, which agrees well with the above calculated electric charge. Similar results had been obtained for other poling conditions. This leads to the conclusion that, under some poling conditions, the electric current measured during the process is due to the displacement of sodium, calcium, and oxygen ions in the glass sample.

The light emitted during the poling procedures is attributed to the breakdown of some chemical bonds by the action of the high electric field and high temperature. This results in electronic transitions that promote the emission of light. It has been observed that the change in the light intensity is intimately related to the variation in the measured electric current. The light is no longer visible 10 min after the start of poling (at 200 °C) and when the current is less than 0.7 mA. The phenomenon is not related to dielectric breakdown, which had actually been observed for higher electric fields, and which was accompanied by a fast increase in the electric current up to higher than 10 mA, which is the upper current limit of the power supply. Moreover, the sparks accompanying electric breakdown occurs persistently at defined places, creating microchannels between the electrodes that can be further observed visually if the voltage is applied some minutes after the occurrence of the breakdown. The phenomenon of light emission during poling has already been mentioned by Moura *et al.*[16]

Adhesion of the anode metal to the glass sample occurred during all poling procedures. The origin of this adhesion can be electrostatic and chemical. The high electric field at the interface of the anode and the glass surface, now with a depletion layer, provides the strong observed adhesion between the anode metal and the glass surface. The chemical origin of the adhesion is the chemical reaction that occurs between the iron or aluminum of the anode and the oxygen ions resulting from reactions (2a) and (2b), thus forming oxides that are incorporated into the near-surface glass composition. The phenomenon is known as anodic adhesion and was recently reviewed by Knowles and van Helvoort.[17]

The changes in the infrared spectra (Fig. 4) of the anodic surface are much more pronounced than that of the cathodic one, indicating that the glass structure near the anode has been highly modified. Taking into account the compositional changes that were observed by EDS measurements, as in Fig. 3, it should be expected that the structural changes observed by infrared spectroscopy are related to those compositional variations. The band in the 760–820 cm$^{-1}$ range undergoes the most pronounced change. The low intensity band at 765 cm$^{-1}$ of the pristine glass shifts to 818 cm$^{-1}$ after poling. This band is attributed to the bending vibration of the Si–O–Si bonds with the oxygen oscillating along the axis bisecting the angle of this bond.[13,18] According to Galeener *et al.*[19] the frequency of this vibrational mode is given by

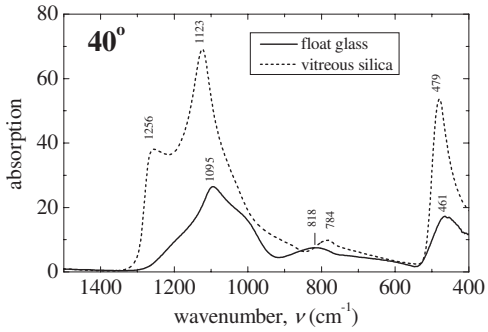


FIG. 11. Specular reflectance of anodic surfaces of poled float glass and vitreous silica, for incidence angle of 40°. Poling conditions: 2 kV, 250 °C, and 20 min, for float glass and 3.5 kV, 280 °C, 90 min, for vitreous silica. The spectra are not normalized.

$$\omega_3^2 = \frac{k}{m_O}(1+\cos\alpha) + \frac{4}{3}\frac{k}{m_{Si}}, \tag{3}$$

where $k$ is the central Born-force constant, $m_O$ and $m_{Si}$ are the masses of oxygen and silicon, respectively, and $\alpha$ is the most probable value of the Si–O–Si bond angle. Based on Raman spectroscopy and inelastic neutron scattering experimental values obtained for vitreous silica, they determined that $k=545$ N/m and $\alpha=130°$. Since $m_O=2.66\times10^{-26}$ kg and $m_{Si}=4.66\times10^{-26}$ kg, in order to obtain $\tilde{\nu}_3=\omega_3/(2\pi c)=765$ cm$^{-1}$, where $c$ is the velocity of light in vacuum, $\alpha$ should be ~138°. With the shift of this band to 816 cm$^{-1}$, due to poling, the angle should have decreased to ~128°, according to Eq. (3). However, the mean value of $\alpha$ in vitreous silica is 144°,[20] which is higher than the calculated angle for the poled float glass. The corresponding infrared band in vitreous silica occurs at about 780 cm$^{-1}$.[21] Thus, although the concentrations of Na and Ca in the anodic surface are drastically reduced after poling, the infrared spectra of the poled float glass are far from being similar to that of vitreous silica.

We performed infrared spectroscopy in poled vitreous silica (Quartzglas, HER 1, Heraeus, 2 mm thick) in order to identify which structural changes can take place in a glass with alkali concentration in the ppm range. The poling was performed at 280 °C for 90 min and with an applied voltage of 3.5 kV. The specular reflectance spectra for incidence angle at 40° of the anodic surface of vitreous silica and float glass are shown in Fig. 11. It was observed that the spectra of the pristine and poled vitreous silica samples show no difference, except for a small intensity decrease in the band at 1256 cm$^{-1}$ after poling. Therefore, there are strong evidences that the shift in the 765 cm$^{-1}$ band to a higher frequency after the poling of float glass is attributed to structural changes related to the decrease in cations ($Na^+$ and $Ca^{2+}$) and $O^-$ concentration at the anodic surface.

Infrared spectra of vitreous silica present the characteristic longitudinal and transversal optical modes, known as TO-LO splittings.[22] The most pronounced of these splittings is that related to the bands at 1123 and 1256 cm$^{-1}$ (Fig. 11), corresponding to the TO and LO modes, respectively, of asymmetric stretching vibrations of the bridging oxygens in the Si–O–Si bonds.[18] The DRIFT spectra of float glass in Fig. 4 show that this splitting is very weak, possibly due to a lower interconnectivity than that of vitreous silica. The relative intensity of the shoulder at ~1180 cm$^{-1}$ of the float glass, related to the TO mode, decreases and the band at 1072 cm$^{-1}$, related to the LO mode, simultaneously shifts to 1100 cm$^{-1}$ after poling. This shift is generally related to the increase in the bridging oxygen concentration in silicate glasses[23] which, in the depleted layer, follows the reaction Eqs. (2a) and (2b). Similar changes in the vibrational structure of the anodic surface of alkali-lead silicate glass had earlier been observed by Carlson *et al.*[3]

Furthermore, there is a narrowing of the most intense band centered at 1070 cm$^{-1}$ (Fig. 4). This narrowing may be attributed to an increase in the ordering degree of the anode glass structure. Nazabal *et al.*,[24] based on their studies of the structure of poled vitreous silica, already proposed that there is a structural anisotropy in the anodic surface attributed to the orientation of the formed $Si-O^-$ groups parallel to the dc field during poling. A strong anisotropy of the microstructure in the anodic surface using SEM was observed by An and Fleming,[6] which they attributed to a phase separation process.

Figure 7 shows that the static contact angle $\theta$ increases as the poling time increases. Some conclusions about the causes that lead the anode to become hydrophobic can be made by analyzing Young's equation:

$$\cos\theta = \frac{\gamma_{sv}-\gamma_{sl}}{\gamma_{lv}}, \tag{4}$$

where $\gamma_{ij}$ are the interfacial energies between media $i$ and $j$, and the subscripts $s$, $l$, $v$ are related to the solid, liquid, and vapor/gas, respectively. Considering that the surface tension of water, $\gamma_{lv}$, is constant, then $\theta$ will increase only if the difference $(\gamma_{sv}-\gamma_{sl})$ decreases. Thus, the poling procedure affects the solid-vapor and solid-liquid interfacial energies. However, according to Eq. (4), for an increase in $\theta$ to take place, there should be an increase in $\gamma_{sl}$ and/or a decrease in $\gamma_{sv}$. This agrees with the statement that low-energy solid surfaces are hydrophobic.[25,26] The behavior observed in Fig. 7 can be attributed to an increase in the induced charge density at the anodic surface and it agrees with experimental results obtained recently by Aronov *et al.*[27] for low-energy electron irradiation of vitreous silica surfaces. Therefore it can be concluded that the observed increase in hydrophobicity of the anodic float glass surface is mainly due to an excess of negative electric charge density on this surface as a result of the $Si-O^-$ dipole orientation with the applied electric field.

The decrease in the refractive index of the anodic surface (Fig. 8) can be explained by the reduction in the concentration of cations with high electronic polarizability, as is the case of $Na^+$ and $Ca^{2+}$, and of nonbridging oxygens, which has yet higher polarizability.[28,29] An additional cause for this decrease is a more open glass structure and consequently a lower density of this surface. Moreover, the presence of small concentrations of MgO and $Al_2O_3$ also impedes reaching a refractive index value as low as that of vitreous silica, $n_D=1.4581$.[30]

## V. CONCLUSION

The analysis of the results of the electric current curves gave strong evidences that not only $Na^+$ but also $Ca^{2+}$ and $O^-$ ions migrate in the glass during thermal poling of soda-lime glass. As a consequence, structural changes accompany those chemical changes. The occurrence of structural changes was detected by infrared spectroscopy. Comparison of infrared spectra of poled float glass and vitreous silica shows that the structural changes in poled vitreous silica are much less pronounced than those occurring in float glass, which leads to the conclusion that the displacement of $Na^+$, $Ca^{2+}$, and $O^-$ causes these changes. The high intensity electric field applied acts on the $Si-O^-$ electric dipoles that, also under the influence of the elevated temperatures, are oriented parallel to the field, resulting in a net negative charge density at the anodic surface. As a consequence, the contact angle increases, which leads the anodic surface to become hydrophobic.

## ACKNOWLEDGMENTS

The authors are grateful to Dr. E. W. Kitajima (NAP-MEPA, ESALQ-USP) for the MEV-EDS facilities, to Dr. Sandra M. M. Franchetti (DBM-IB-UNESP) for the DRIFT facilities, and to Dr. S. J. L. Ribeiro and Dr. M. A. U. Martines (IQ-UNESP) for specular reflectance infrared facilities. Helpful discussion with Dr. D. L. Chinaglia and Dr. R. A. Moreno Alfaro (DF-IGCE-UNESP) are greatly acknowledged. The poled vitreous silica samples were kindly supplied by Dr. Isabel C. S. Carvalho (PUC-Rio). This research was supported by FAPESP (Grant Nos. 05/00599-3, 05/04397-6, and 07/02931-0).

[1]R. A. Myers, N. Mukherjee, and S. R. J. Brueck, Opt. Lett. **16**, 1732 (1991).
[2]D. E. Carlson, J. Am. Ceram. Soc. **57**, 291 (1974).
[3]D. E. Carlson, K. W. Hang, and G. F. Stockdale, J. Am. Ceram. Soc. **57**, 295 (1974).
[4]U. K. Krieger and W. A. Lanford, J. Non-Cryst. Solids **102**, 50 (1988).
[5]C. M. Lepienski, J. A. Giacometti, G. F. Leal Ferreira, F. L. Freire, Jr., and C. A. Achete, J. Non-Cryst. Solids **159**, 204 (1993).
[6]H. An and S. Fleming, J. Opt. Soc. Am. B **23**, 2303 (2006).
[7]See http://www.abividro.org.br/index.php/19, retrieved 2 December 2006.
[8]L. A. B. Pilkington, Proc. R. Soc. London, Ser. A **314**, 1 (1969).
[9]J. S. Sieger, J. Non-Cryst. Solids **19**, 213 (1975).
[10]G. H. Frischat, C. R. Chim. **5**, 759 (2002).
[11]J. Deubener, R. Brückner, and H. Hessenkemper, Glastech. Ber. **65**, 256 (1992).
[12]I. Šimon and H. O. McMahon, J. Am. Ceram. Soc. **36**, 160 (1953).
[13]B. C. Trasferetti and C. U. Davanzo, Appl. Spectrosc. **54**, 502 (2000).
[14]C. Z. Tan, J. Phys. Chem. Solids **63**, 179 (2002).
[15]M. Qiu, F. Pi, G. Orriols, and M. Bibiche, J. Opt. Soc. Am. B **15**, 1362 (1998).
[16]A. L. Moura, M. T. de Araujo, E. A. Gouveia, M. V. D. Vermelho, and J. S. Aitchison, Opt. Express **15**, 143 (2007).
[17]K. M. Knowles and A. T. J. van Helvoort, Int. Mater. Rev. **51**, 273 (2006).
[18]R. M. Almeida, Phys. Rev. B **45**, 161 (1992).
[19]F. L. Galeener, A. J. Leadbetter, and M. W. Stringfellow, Phys. Rev. B **27**, 1052 (1983).
[20]R. L. Mozzi and B. E. Warren, J. Appl. Crystallogr. **2**, 164 (1969).
[21]R. M. Almeida, T. A. Guiton, and C. G. Pantano, J. Non-Cryst. Solids **119**, 238 (1990).
[22]F. L. Galeener and G. Lucovsky, Phys. Rev. Lett. **37**, 1474 (1976).
[23]P. E. Jellyman and J. P. Procter, J. Soc. Glass Technol. **39**, 173 (1955).
[24]V. Nazabal, E. Fargin, G. Le Flem, V. Brois, C. Cartier dit Moulin, T. Buffeteau, and B. Desbat, J. Appl. Phys. **88**, 6245 (2000).
[25]P. G. de Gennes, Rev. Mod. Phys. **57**, 827 (1985).
[26]C. W. Extrand and Y. Kamagai, J. Colloid Interface Sci. **191**, 378 (1997).
[27]D. Aronov, M. Molotskii, and G. Rosenman, Phys. Rev. B **76**, 035437 (2007).
[28]H. Scholze, *Glass—Nature Structure, and Properties* (Springer-Verlag, New York, 1991).
[29]J. E. Shelby, *Introduction to Glass Science and Technology* (The Royal Society of Chemistry, Cambridge, 1997).
[30]P. Chindaudom and K. Vedam, Appl. Opt. **32**, 6391 (1993).